

FIRST DEMONSTRATION OF A GaInP/GaAs HBT YIG-TUNED MICROWAVE OSCILLATOR

S.J.Prasad and C.Haynes

Electronics Research Labs
Tektronix, MS 50-324, Beaverton, OR 97077, USA.

ABSTRACT

A YIG-tuned oscillator using GaInP/GaAs HBT as the active device is described. The oscillator can be tuned from 6 to 9GHz. The f_T and f_{max} of the HBT was 42 and 33GHz respectively. At 7.8GHz, the phase noise of the oscillator was -85dBc/Hz at 10kHz offset from the carrier. These results compare very well with the phase noise data available for AlGaAs/GaAs HBT oscillators.

INTRODUCTION

Microwave oscillators have traditionally used bipolar transistors or GaAs MESFETs as the active device. Recently, there has been a considerable interest in AlGaAs/GaAs and SiGe HBT oscillators [1-7]. Most of the oscillators reported so far use AlGaAs/GaAs HBTs along with a dielectric resonator (DRO) or simply use L-C type circuits for producing oscillations. Yttrium-Iron-Garnet (YIG) resonators have very high Q's and can be easily tuned over a broadband with an applied magnetic field. To date, there have been no reports of YIG-tuned oscillators using HBTs. This paper describes a 6-9GHz YIG-tuned oscillator using the newly developed GaInP/GaAs HBT.

GaInP/GaAs HBT TECHNOLOGY

Though the AlGaAs/GaAs HBT technology has matured, it is not the best material system for realizing high current gain. The GaInP/GaAs system provides a small conduction-band offset and a large valence-band offset which is essential for realizing high gain HBTs. In addition, the growth of AlGaAs/GaAs structures is very difficult due to gettering of oxygen by aluminum. Unlike AlGaAs/GaAs, wet chemical processing of GaInP/GaAs structures is simple due to the availability of selective chemical etchants. The AlGaAs emitter contains traps (DX centers) whereas the GaInP emitter is free from traps making it the material of choice for HBTs. The epitaxial structure for our HBTs was grown at Epitronix Corporation and had a p-type carbon doped GaAs base ($4 \times 10^{19} \text{ cm}^{-3}$, $0.05 \mu\text{m}$). The emitter consisted of n-type GaInP $0.1 \mu\text{m}$ thick doped to $5 \times 10^{17} \text{ cm}^{-3}$. The devices were fabricated using a triple mesa

etch process in use at Tektronix for fabricating analog and digital HBT ICs. Microwave measurements were

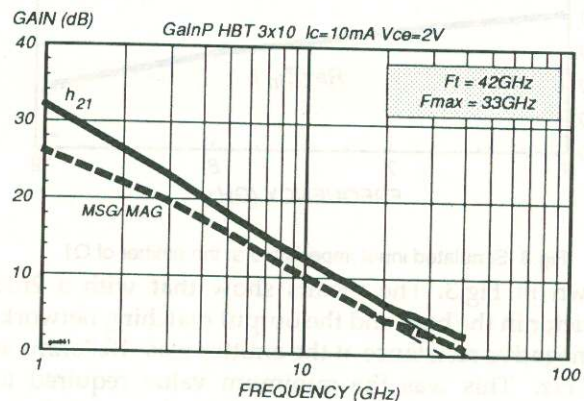


Fig.1. High frequency performance of $3 \mu \times 10 \mu$ HBT.

made on $3 \times 10 \mu^2$ HBTs biased at $I_C = 10 \text{ mA}$ and $V_{CE} = 2 \text{ V}$ and the results are shown in Fig.1. By extrapolating the current gain h_{21} and the maximum available gain (MAG) we obtain an f_T of 42GHz and an f_{max} of 33GHz.

DESIGN TECHNIQUES

The oscillator design was carried out [8,9] using the measured S-parameters. A schematic of the YIG oscillator is shown Fig.2. A single emitter $3 \mu \times 10 \mu$

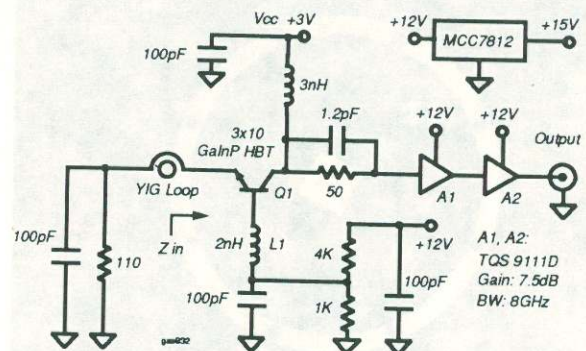


Fig.2. YIG oscillator circuit.

GaInP/GaAs HBT was used for Q1 with the measured characteristics as shown in Fig.1. In the 6-9GHz range, the device has a MAG >10dB making it possible to design an oscillator. The HBT Q1 was operated in the

common-base mode to make the stability factor $K < 1$. A 1mil thick bond wire used for the base had an inductance L_1 of 2nH which provided the required negative resistance. The resonator consisted of a YIG sphere 10mil in diameter and a 3/4 turn loop using 3mil thick gold wire. Computer simulations of the input impedance Z_{in} looking into the emitter of the HBT is

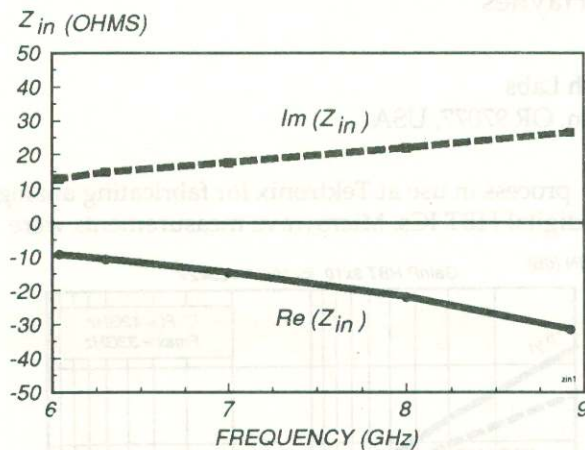


Fig.3. Simulated input impedance at the emitter of Q1.

shown in Fig.3. The results show that with a 2nH inductor in the base and the output matching network, the negative resistance at the emitter was -10.7ohms at 6.3GHz. This was the minimum value required to compensate for losses in the YIG sphere and the

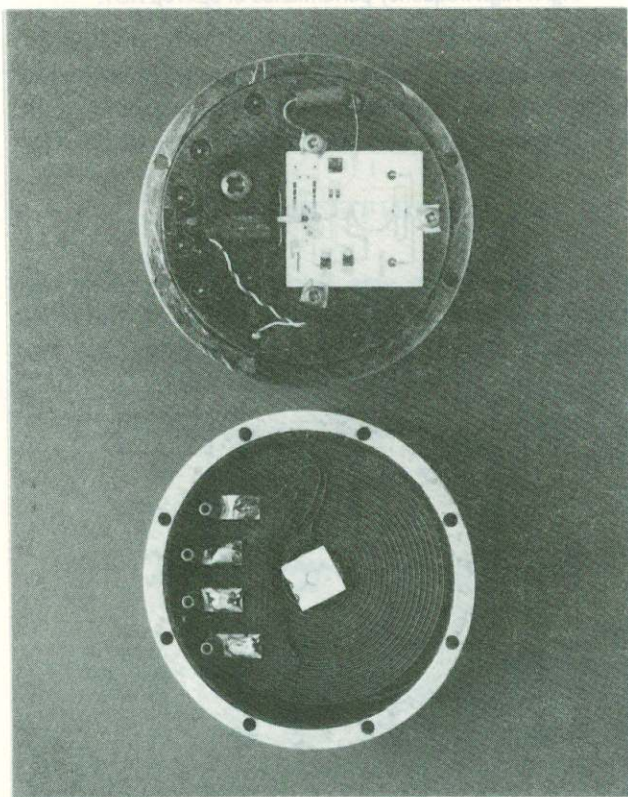


Fig.4. Photograph of the YIG oscillator assembly.

coupling loop. In addition, the reactive part of the input impedance looking into emitter of Q1 was maintained inductive to avoid spurious oscillations. The amplifiers A1 and A2 are GaAs MESFET distributed amplifiers (TriQuint TQS 9111D) and each had a gain of 7.5dB and bandwidth of 8GHz. The maximum frequency of oscillation was 9GHz, which was mainly limited by the 8GHz bandwidth of the amplifiers A1 and A2. The 4k Ω - 1k Ω voltage divider maintained the base at 2.4V. Allowing for a V_{BE} drop of 1.3V, the emitter was maintained at 1.1V setting the collector current to 10mA. To keep the device biased close to the measurement conditions in Fig.1, the supply voltage V_{CC} was set to 3V so that V_{CE} was 1.9V. Fig.4 is the inside view of the YIG oscillator showing various components. The HBT was die attached to the alumina substrate and the bond wire formed inductor L_1 . The hybrid also had a Wilkinson power divider at the output of A2 with a 2 to 1 power split which is not shown in the schematic for simplicity. The voltage regulator chip MCC7812 provided the 12V needed for the amplifiers A1 and A2 and the 15V supply powered the heater for the YIG sphere.

EXPERIMENTAL RESULTS

The tuning range of the oscillator was from 6.3 to 8.8GHz. The low-end was limited by the -10.7 ohms negative resistance that was required to compensate the losses in the YIG resonator circuit. Due to layout considerations, the bond wire length could not be adjusted and the oscillator could not be tuned to lower frequencies. Typical output spectrum at 8.8GHz is shown in Fig.5. The output power in Fig.5 is about 12dB lower than the oscillator output due to power splitters used to simultaneously monitor power and frequency.

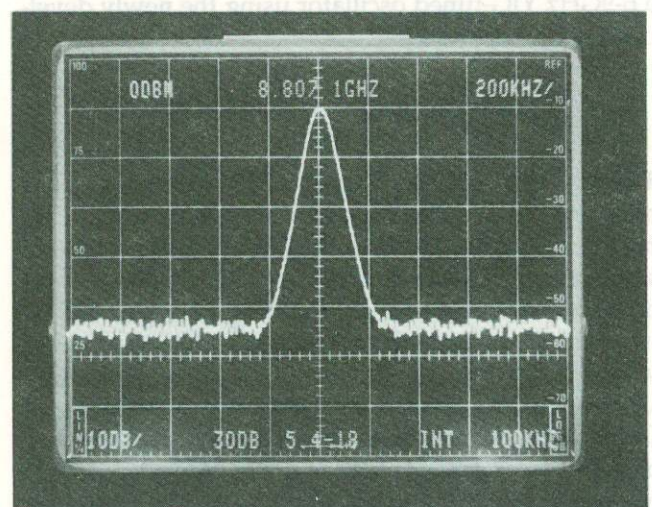


Fig.5. Output spectrum from the YIG oscillator.

The power vs frequency curve is shown in Fig.6. The power dropped off rapidly due to the 8GHz bandwidth

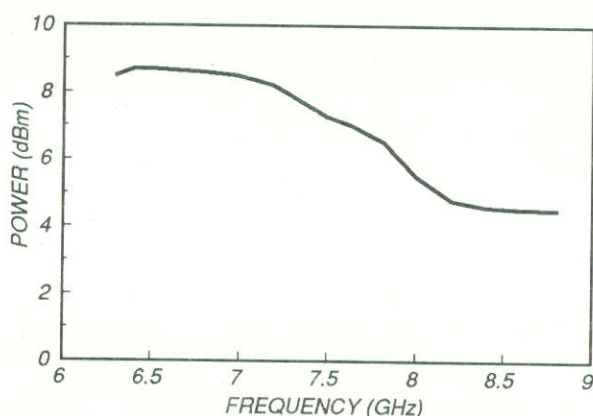


Fig.6. Output power vs frequency curve.

limitation of A1 and A2. Due to low output power, phase noise measurements could not be made at 8.8GHz. However, phase noise measurements were performed at 7.78GHz using the delay line-discriminator method. The phase noise showed a $1/f^3$ dependence at low frequencies and a $1/f^2$ dependence beyond 50kHz offset from the carrier indicating a $1/f$ noise corner frequency of approximately 50kHz. From Fig.7, we notice that the phase noise is -85dBc/Hz at

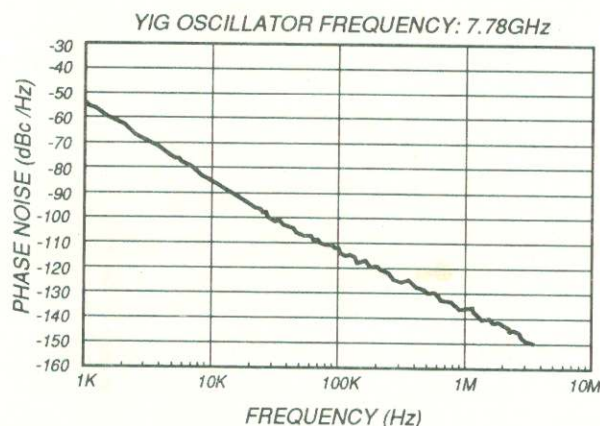


Fig.7. Phase noise data at 7.8GHz

10kHz offset from the carrier. The phase noise of the present oscillator compares well with the published phase noise results of other HBT oscillators shown in Table.1. These results show that GaInP/GaAs HBTs do not have any additional noise mechanisms compared to AlGaAs/GaAs HBTs. The oscillator had a second harmonic component of -40dBc and spurious signals were below -60dBc. To verify the stability of the oscillator, the supply voltage V_{CC} was varied from 2.5V to 3.5V and the change in frequency was 3MHz with the oscillator running at 7.8GHz.

CONCLUSION

We have demonstrated a GaInP/GaAs HBT YIG tuned oscillator tunable from 6 to 9GHz. Phase noise measurements at 7.78GHz show that the phase noise is -85dBc/Hz when offset from the carrier by 10kHz.

ACKNOWLEDGMENT

The authors would like to thank L.Lockwood for phase noise measurements and B.Murdock for encouragement and support.

REFERENCES

1. K.K.Agarwal, "Dielectric Resonator Oscillators using GaAs/AlGaAs HBTs" IEEE MTT-S digest, pp.95-98, 1986.
2. N.Hayama et al., "A Low-Noise Ku Band AlGaAs/GaAs HBT Oscillator", IEEE MTT-S Digest, pp.679-682, 1988.
3. M.E.Kim et al., "12-40GHz Low Harmonic Distortion and Phase Noise of GaAs Heterojunction Bipolar Transistors", GaAs IC Symposium Digest, pp.117-120, 1988.

Table.1. Phase noise data for various AlGaAs/GaAs HBT Oscillators.

Circuit	Osc.Freq (GHz)	Phase Noise dBc/Hz	Offset kHz	Ref
4GHz DRO	4.0	-95	10	1
Ku-Band HBT Oscillator	15.5	-65	10	2
27-43GHz Oscillator	29.0	-80	100	3
X band HBT DRO	12.3	-70	10	4
25GHz DRO	24.8	-78	10	5
15GHz VCO	15.1	-85	100	6
Si-SiGe HBT DRO	9.6	-85	100	7

4. M.A.Khatibzadeh et al., "High Power and High Efficiency Monolithic HBT VCO Circuit", GaAs IC Symposium Digest, pp.11-14, 1989.
5. K.Ogawa et al., "25GHz Dielectric Resonator Oscillator Design using an AlGaAs/GaAs HBT", Electronics Letters, 26(18), pp.1514-1516, 1990.
6. Y.Yamauchi et al., "A 15GHz Monolithic Low Phase Noise VCO using AlGaAs/GaAs HBT", GaAs IC Symposium Digest, pp.259-262, 1991.
7. U.Guttich et al., "A Si-SiGe HBT Dielectric Stabilized Microstrip Oscillator at X-Band Frequencies", IEEE MGW 2(7), pp.281-283, 1992.
8. G.R.Basawapatna and R.B.Stancliff, "A Unified Approach to the Design of Wide-Band Microwave Solid-State Oscillators", IEEE Trans. MTT 27(5), pp.379-385, 1979.
9. J.C.Papp and Y.Y.Koyano, "An 8-18GHz YIG-Tuned FET Oscillator", IEEE Trans. MTT 28(7), pp.762-767, 1980.

ACKNOWLEDGMENT

The author would like to thank L. L. Chua for his helpful discussions and R. B. Stancliff for his encouragement.

REFERENCES

1. J. C. Papp and Y. Y. Koyano, "An 8-18GHz YIG-Tuned FET Oscillator", IEEE Trans. MTT 28(7), pp.762-767, 1980.
2. G. R. Basawapatna and R. B. Stancliff, "A Unified Approach to the Design of Wide-Band Microwave Solid-State Oscillators", IEEE Trans. MTT 27(5), pp.379-385, 1979.
3. M. A. Khatibzadeh, "High Power and High Efficiency Monolithic HBT VCO Circuit", GaAs IC Symposium Digest, pp.11-14, 1989.

The curves are frequency in Hz vs. time in Fig. 5. The curves are plotted on a log scale.



The curves are frequency in Hz vs. time in Fig. 6. The curves are plotted on a log scale. The curves show a similar trend to Fig. 5, with a rapid increase in frequency followed by a steady state.



Fig. 6. Frequency vs. time.

Time (ns)	Frequency (Hz)	Power (dBm)	Phase (deg)	Modulation (dB)
0	10	10	0	0
10	10	10	0	0
100	100	100	0	0
10	10	10	0	0
10	10	10	0	0
100	100	100	0	0
10	10	10	0	0